RARE METALS
Vol. 31, No. 6, Dec. 2012, p. 531
DOI: 10.1007/s12598-012-0552-1

Microstructure and tensile properties of low cost titanium alloys at different cooling rate

WANG Guo, HUI Songxiao, YE Wenjun, MI Xujun, WANG Yongling, and ZHANG Wenjing

State Key Laboratory for Fabrication & Processing of Nonferrous Metals, General Research Institute for Nonferrous Metals, Beijing 100088, China

Received 3 July 2012; received in revised form 25 July 2012; accepted 30 August 2012

Abstract

Titanium and titanium alloys have several advantages, but the cost of titanium alloys is very expensive compared with the traditional metal materials. This article introduces two new low-cost titanium alloys Ti-2.1Cr-1.3Fe (TCF alloy) and Ti-3Al-2.1Cr-1.3Fe (TACF alloy). In this study, we used Cr-Fe master alloy as one of the raw materials to develop the two new alloys. We introduce the microstructure and tensile properties of the two new alloys from β solution treated with different cooling methods. Optical microscopy (OM), X-ray diffractometry (XRD), and transmission electron microscopy (TEM) were employed to analyze the phase constitution, and scanning electron microscopy (SEM) was used to observe the fracture surfaces. The results indicate that the microstructures consist of β grain boundary and α′ martensite after water quenching (WQ), β matrix and α phase after air cooling (AC) and furnace cooling (FC), respectively. Also, the microstructure is the typical basketweave structures after FC. Of course, athermal ω is also observed by TEM after WQ. The strength increases with decreasing cooling rates and the plasticity is reversed. Because of the athermal ω, the strength and ductility are highest and lowest when the cooling method is WQ. The strength of TACF alloy is higher than the TCF alloy, but the plasticity is lower. The fracture surfaces are almost entirely covered with dimples under the cooling methods of AC and FC. Also, we observe an intergranular fracture area that is generated by athermal ω, although some dimples are observed after WQ.

Keywords: titanium alloys; microstructure; martensite; tensile properties; fracture morphology

1 Introduction

The use of titanium alloys in automobile parts is because of their high specific strength, good hardenability, excellent fatigue and crack-propagation behavior, half elastic modulus of steel, low thermal expansion coefficient, nonmagnetic, manufacturability and no pollution to environment, etc [1–3]. For these advantages, titanium alloys are used as automobile materials, and it can lower the weight of car, reduce fuel consumption, increase efficiency, improve environment and reduce noise, etc. [4–5]. However, their applications to automobile parts are limited to racing and special-purpose cars because of their high cost [4]. High cost hinders the application of titanium alloys not only in the automobile industry, but also in other aspects of the civil field [4–6]. Therefore, how to reduce the cost of titanium alloys has become the focus of this study. So far, there are about three successful methods to reduce the cost of titanium alloys [7–9]. First, using cheaper raw materials to design alloys, such as Mo-Fe master alloy and Fe element, etc. [10]; second, improve the characteristics; lastly, improve the material utilization during the material processing. In America, they developed Timetal 62S (Ti-6A1-2Fe-0.1Si) alloy and Timetal LCB (Ti-4.5Fe-6.8Mo-1.5Al) alloy through using Fe element or Fe-Mo master alloy to replace the V element respectively [11]; In Japan, they developed Ti-0.05Pd-0.3Co through using Co element to replace part Pd of Ti-0.2Pd alloy [12]; In China, Northwest Institute for Non-ferrous Metal Research developed near α alloy Ti8LC (TiAlFeMo) and near β alloy Ti12LC (TiAlFeMo) through using Fe-Mo master alloy to replace V element in the TC4 alloy [13].

We developed low-cost Ti-Al-Cr-Fe titanium alloys by using Cr-Fe master alloy for automobile springs, and the price of the Cr-Fe master alloy is cheaper than other raw materials. The cost of the Ti-Al-Cr-Fe alloys is approximately the same as the sponge titanium. Gunawarman B. [14–15] also developed two low-cost β titanium alloys Ti-4.3Fe-7.1Cr and Ti-4.3Fe-7.1Cr-3.0Al for healthcare and medical applications. The low-cost titanium alloys that we developed are new type α/β titanium alloys, so we studied the influence of heat treatment on microstructure and tensile

Corresponding author: HUI Songxiao **E-mail:** huisx@grinm.com

properties.

2 Experimental

The two new titanium alloys used for this study were double melted by the consumable vacuum arc remelting (VAR) 15 kg ingots. The ingots were forged at 1323 K then hot-rolled into bars with 12 mm in diameter at 1223 K. Table 1 shows the composition of the bars in mass fraction. TCF and TACF represent the Ti-2.1Cr-1.3Fe and Ti-3Al-2.1Cr-1.3Fe respectively in the following content. The T_β of the two alloys are (1178±5) K and (1203±5) K through metallographic observation. Samples with Φ12 mm×10 mm and Φ12 mm×70 mm were prepared from hot rolled bar by machining. Each sample was solution treated at T_β+20 K for 30 min and then cooled by one of the three different cooling methods: water quenching (WQ), air cooling (AC) and furnace cooling (FC). After cooling, the metallographic specimens were polished on waterproof abrasive paper such as 240#, 400#, 600#, 800#, 1000#, 1500# and 2000#. The electrochemical finishing method was employed to polish the surfaces. The polishing solution was 95% acetic acid and 5% perchloric acid in volume; the voltage was about 60 to 70 V, the time was about 10 to 20 s. Then etched in etching liquids HF: HNO_3: H_2O=1:3:10 in volume, the corrosion time is about 45 s. Tensile test specimens were machined into a cylindrical shape with 60 mm gage in length and 5 mm in diameter and were tested on an AG-501CNE Testing Machine at a crosshead speed of 1×10^{-3} m·min^{-1} to failure at room temperature. Microstructure and phase constitution were observed by optical microscopy (OM), X-ray diffractometry (XRD), transmission electron microscopy (TEM), and fracture surfaces were observed by scanning electron microscopy (SEM).

3 Results and discussion

3.1 Microstructure characteristic

Figure 1 shows the X-ray diffraction profiles of TCF and TACF alloys cooled by different methods. The β and α reflection were identified cooled by AC and FC and the β phase and α′ martensite were identified cooled by WQ in both alloys. In these samples, β grains, β grain boundary, α phase and α′ martensite were also observed by OM, and they are shown in Fig. 2.

Figures 2(a) and (b) are the OM of both alloys after WQ; they show that the microstructures consist of β boundary and α′ martensite, and the average values of grain size are about 200 to 300 μm and 250 to 600 μm, respectively. Figures 2(c) and (d) are the OM after AC, α phase full of β grains in the two pictures, the average values of grain size are about 150 to 300 μm and 250 to 500 μm, respectively. The average of grain size of TACF is larger than the TCF alloy, we analyzed that the Al element may play an important role in the TACF alloy. Figures 2(e) and (f) are the OM after FC; they show a typical basketweave structure, which consists of intersecting arrangement of α colonies. In Fig. 2, β grains, β grain boundary, α phase and α′ martensite were also observed, which corresponds to the X-ray diffraction results.

There is a significant influence of average cooling rates on the microstructure. When the cooling method is WQ, the high temperature phase has no time to precipitate because of

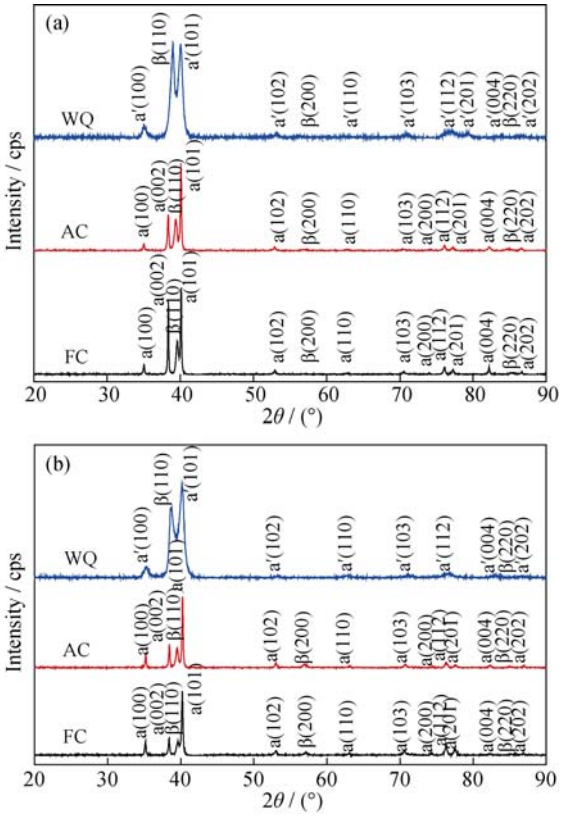

Fig. 1 XRD patterns on various cooling rates from solution treated at T_β+20 K for 30 min
(a) TCF alloy; (b) TACF alloy

Table 1 Compositional analysis of low cost titanium alloys (wt.%)

Elements	Al	Cr	Fe	Si	C	H	O	N
Ti-2.1Cr-1.3Fe (TCF)	–	2.16	1.26	0.0487	0.078	0.0032	0.054	0.0060
Ti-3Al-2.1Cr-1.3Fe(TACF)	2.88	2.08	1.25	0.0533	0.075	0.0037	0.037	0.0046

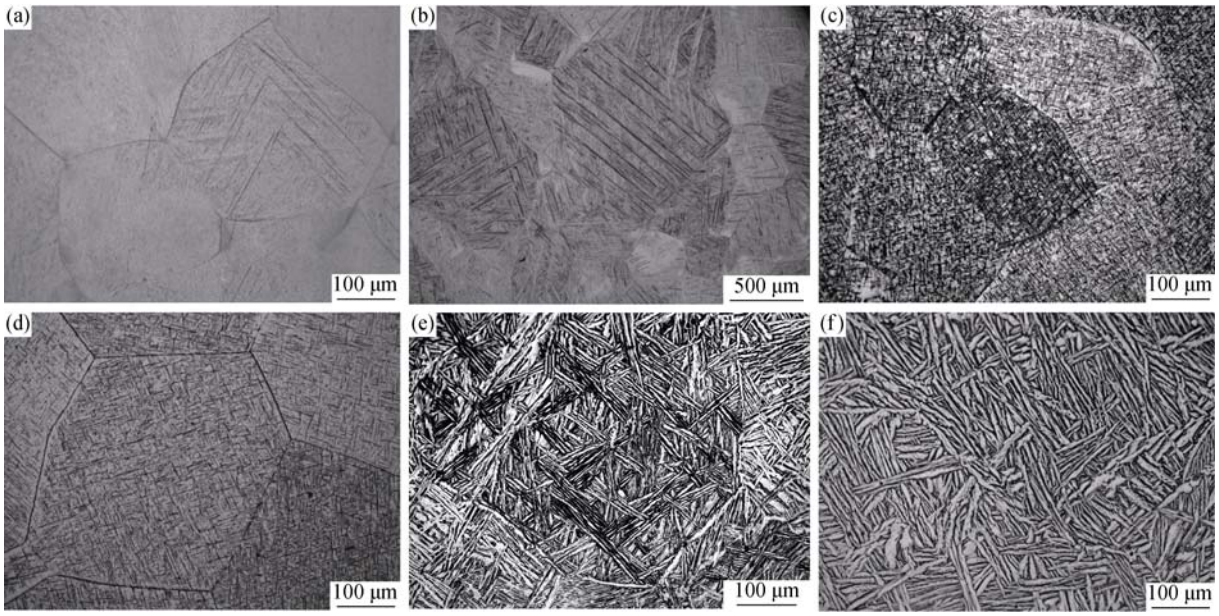

Fig. 2 OM of two alloys after different cooling rates from solution treated at T_β+20 K for 30 min
(a) Cooled by WQ of TCF alloy; (b) Cooled by WQ of TACF alloy; (c) Cooled by AC of TCF alloy; (d) Cooled by AC of TACF alloy; (e) Cooled by FC of TCF alloy; (f) Cooled by FC of TACF alloy

Fig. 3 TEM image of α′ martensite in TACF alloy solution treatment at 1233 K for 30 min after WQ

rapid cooling rate, so the prior β boundary becomes dim in micrograph, and the inner phase turns to the quenching martensite without diffusion shear transformation. That is, a martensitic transformation is a reaction without diffusion of substitutional atoms, which involves a cooperative motion and a shear transformation. In this article, the quenching martensite is α′ martensite; the morphology of α′ martensite is like a tiny needle, which is shown in Fig. 3 [16]. After AC, the grain boundary α and inner α phase precipitate, grain boundary α nucleates and grows along the β boundary, inner α phase presents parallel microstructure shape along some habit planes (Figs. 2(c) and (d)). After FC, the grain boundary α and inner α grow, become coarse and then outburst the β boundary, forming the widmanstaten or basketweave structures (Figs. 2(e) and (f)). We find that the values of grain size of these two alloys are larger than that of Ti-4.3Fe-7.1Cr-3.0Al alloy, which was solution treated at 1123 K for 1h and then cooled to room temperature by using five different cooling methods [17]. The grain size values of the Ti-4.3Fe-7.1Cr-3.0Al alloy increase from 126 to 138 μm with cooling rates changed. We analyze that there are two reasons. First, the solution temperatures are higher in this paper; second, the weight percentage of Cr in Ti-4.3Fe-7.1Cr-3.0Al alloy is higher than in our alloys, and Cr could refine grains in metal materials [18].

However, ω phase is found with small size of several nanometers in both alloys through TEM and relative SAD pattern. Figure 4 shows the dark field images and selected area diffraction of athermal ω phase, and the crystal zone axis are $[011]_\beta$. The ω phase is hard and brittle, and dislocations could not move in it, so it would enhance the strength, hardness and elastic modulus. However, the plasticity of alloys decrease rapidly with increasing volume fraction of ω phase [19].

3.2 Tensile properties

Figure 5 shows the trends in tensile strength R_m, yield strength $R_{p0.2}$, elongation A and reduction in area Z with various cooling rates from β solution treatment of the two alloys. Table 2 shows the data characterizing tensile properties. Figure 5 and Table 2 indicate that the strength is enhanced and the plasticity decreases with increasing cooling rates for both alloys.

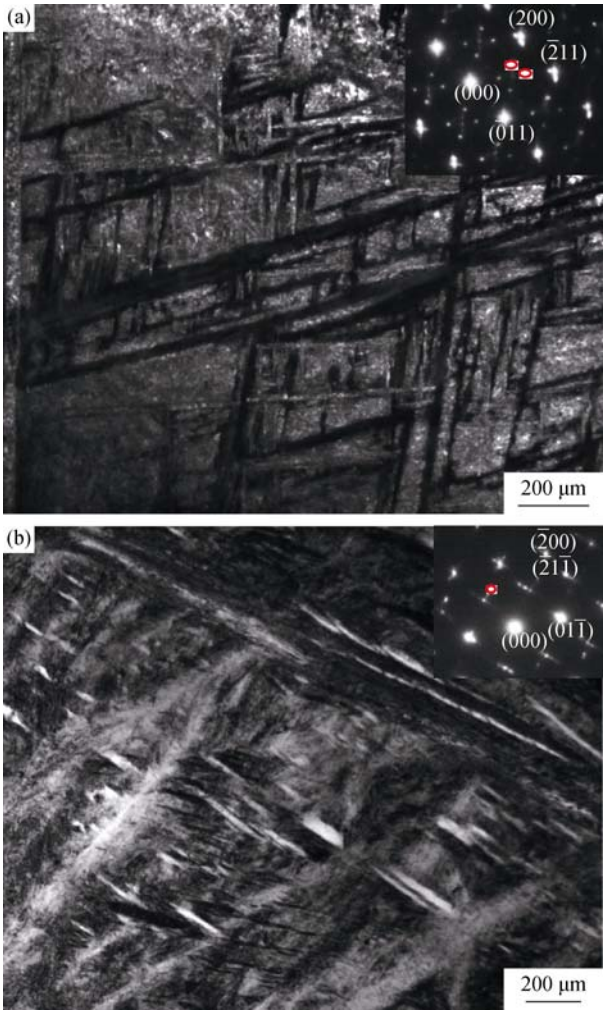

Fig. 4 Dark field TEM images of ω phase and selected diffraction of both alloys from solution treatment at T_β+20 K for 30 min after WQ
(a) TCF alloy; (b) TACF alloy

Under the same heat treatment condition, the strength of TACF alloy is higher than that of TCF alloy, and the plasticity of TACF alloy is lower than that of TCF alloy. The tensile strength of TCF is 94% of the TACF alloy after WQ, 83.5% and 80% after AC and FC, respectively. Elongation A and reduction in area Z of TCF alloy increase dramatically with further decreasing of the cooling rate and then decrease slightly with decreasing cooling rate. The trend of reduction in area Z of TACF alloy is the same as TCF alloy. The trend of elongation A is increased dramatically with decreasing cooling rate and then increased slightly with further decreasing cooling rate.

In the case of TACF alloy, the highest tensile strength and yield strength are 1235 MPa and 1130 MPa respectively, which are obtained cooled by WQ. However, elongation A and reduction in area Z of the alloy cooled by WQ are only 2.5% and 4.5%, respectively. The good strength and good

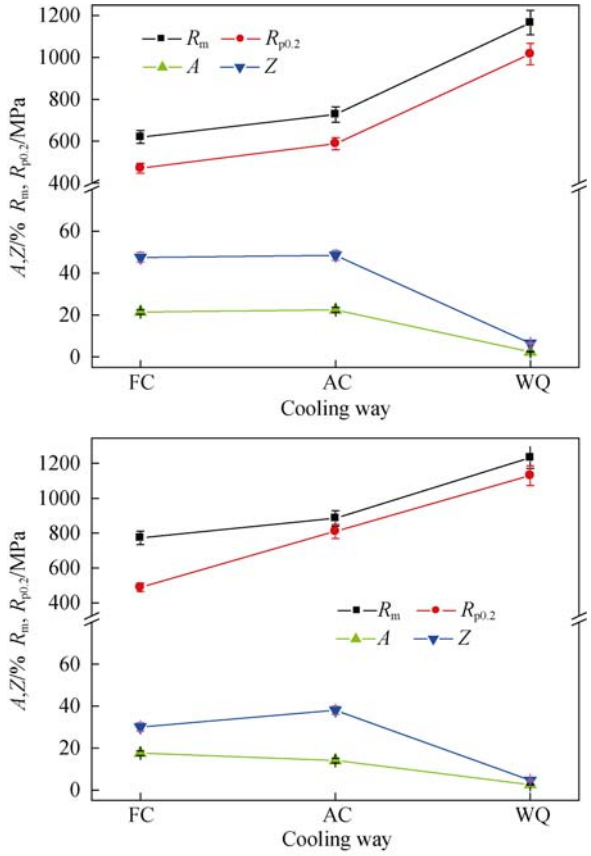

Fig. 5 Tensile properties on various cooling rates from solution treatment at T_β+20 K for 30 min
(a) TCF alloy (b) TACF alloy

Table 2 Value of tensile properties of alloys

Cooling ways	Alloy	R_m/ MPa	$R_{p0.2}$/MPa	A/%	Z/%
WQ	TCF	1165	1015	2.5	6.5
	TACF	1235	1130	2.5	4.5
AC	TCF	730	590	22.5	48.5
	TACF	885	810	14.0	38.0
FC	TCF	620	470	21.5	47.5
	TACF	775	490	17.5	30.0

Table 3 Typical properties of Ti-6Al-4V [2]

Heat treatment	R_m/ MPa	$R_{p0.2}$/MPa	A/%	Z/%
700~800°C/1~3h/AC	>890	>825	>10	>25

plasticity are obtained simultaneously in the TACF alloy cooled by AC. The tensile properties of TACF alloy cooled by AC are approximate to those of Ti-6Al-4V alloy, which are shown in Table 3.

Figure 5 also shows that the strength of TACF alloy is higher than that of TCF alloy. This is because the TACF alloy includes Al element. As one of the α stable elements, Al could increase the T_β, augment the area of α phase, increase

the amount of α phase at some heat treatments, so it could enhance the strength of the alloy, and at the same time, reduce the plasticity of the alloy [20]. In addition, Al plays a significant role in solution strengthening in titanium alloys after solution treatment, which could enhance the tensile strength and yield strength. The study indicated that the addition of 1 wt.% Al element could increase the strength about 50 MPa and decrease the plasticity by about 5% [13]. The result of this article is similar to others' research, but the amplitude is small, which may result from the interaction of Al-Cr or Al-Fe.

There is an interesting piont. In the Ref. [14], the highest strength was obtained in the alloy cooled by FC, which is quite the opposite to our research results. According to TEM analysis, we found that the athermal ω phase forms in both alloys cooled by WQ. The athermal ω phase is hard and brittle, and it could enhance the strength, hardness and elastic modulus, which accounts for the highest tensile strength and the lowest ductility of the alloys cooled by WQ in our research.

3.3 Fracture analysis

Figure 6 shows the SEM micrographs of fracture morphology of tensile samples. Dimples are observed in the samples cooled by different cooling methods (WQ, AC and FC). The fracture surfaces of tensile samples cooled by AC and FC are almost entirely covered with dimples. This situation supports the tensile test results, e.g., tensile strength R_m is about 885 MPa, yield strength $R_{p0.2}$ is about 810 MPa, elongation A is above 14% and reduction in area Z is above 38% cooled by AC of TACF alloy. There are more dimples in Fig. 6(c) than in Fig. 6(f). It suggests that the plasticity of TCF alloy is better than that of TACF alloy under the same heat treatment condition. On the fracture surfaces of the tensile samples cooled by WQ, an intergranular fracture area and some dimples are observed (Figs. 6(a) and (b)). This accounts for the tensile properties of the water quenching samples such as low elongation and low reduction in area in Fig. 5.

4 Conclusion

The phase constitution and tensile properties of Ti-2.1Cr-1.3Fe and Ti-3Al-2.1Cr-1.3Fe alloys from beta solution treatment were investigated by OM, XRD, TEM and SEM. In the samples cooled by different methods, α phase, β phase and α′ martensite are identified by XRD. Also, athermal ω phase is observed by TEM and relative SAD pattern when the cooling method was WQ. Tensile strength R_m and yield strength $R_{p0.2}$ increased with the increasing cooling rate, while the changing trend of elongation A and reduction in area Z is reversed. The strength of Ti-3Al-2.1Cr-1.3Fe alloy is higher than that of Ti-2.1Cr-1.3Fe, but the plasticity is reversed. The highest tensile strength and yield strength are

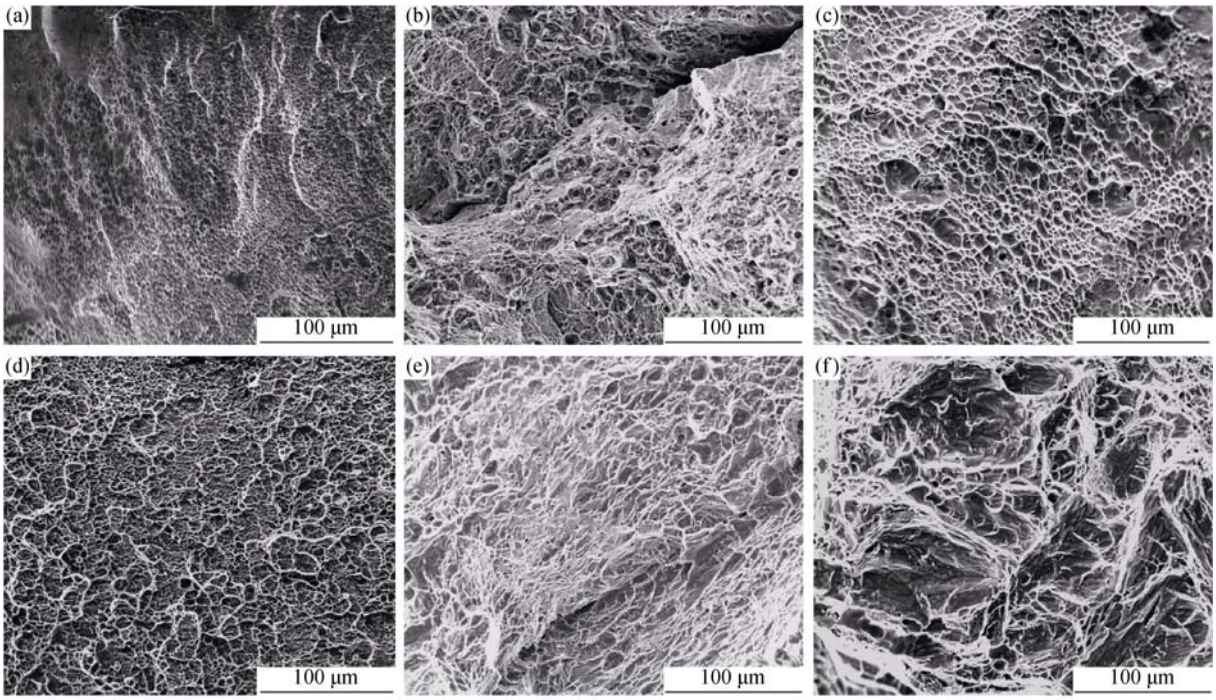

Fig. 6 SEM images of fracture surfaces of alloys cooled by different cooling rates from solution treatment at T_β+20 K for 30 min
(a) SEM image of TCF alloy after WQ; (b) SEM image of TCF alloy after AC; (c) SEM image of TCF alloy after FC; (d) SEM image o of TACF alloy after WQ; (e) SEM image of TACF alloy after AC; (f) SEM image of TACF alloy after FC

1235 MPa and 1130 MPa, respectively, which are obtained in Ti-3Al-2.1Cr-1.3Fe alloy cooled by WQ. However, the plasticity is bad because of the precipitation of athermal ω phase. Ti-3Al- 2.1Cr-1.3Fe alloy cooled by AC shows good strength and good plasticity simultaneously. The fracture surfaces of alloys are covered with dimples when the cooling methods are AC and FC. An intergranular fracture area is also observed, although some dimples are observed cooled by WQ.

Acknowledgement

This article was financially sponsored by the International Science and Technology Cooperation Project (No. 2010DFA52280).

References

[1] Luo J., and Li M.Q., Modeling of grain size in isothermal compression of Ti-6Al-4V alloy using fuzzy neural network, *Rare Met*., 2011, **30** (6): 555.

[2] Liu R., Hui S.X.,Ye W.J., Xiong B.Q.,Yu Y., and Fu Y.Y., Dynamic fracture of TA15ELI alloy studied by instrumented impact test, *Rare Met*., 2010, **29** (6): 608.

[3] Yu Y., Hui S.X., Ye W.J., and Xiong B.Q., Mechanical properties and microstructure of an α+β titanium alloy with high strength and fracture toughness, *Rare Met*., 2009, **28** (4): 346.

[4] Fujii H., Takahashi K., and Yamashita Y., Application of Titanium and its alloys for automobile parts, *Shinnittetsu Giho.*, 2003, (88): 70.

[5] Hartman A. D., Gerdemann S. J., and Hansen J. S., Producing lower-cost titanium for automotive applications, *JOM*, 1998, **50** (9): 16.

[6] Faller K., and (Sam) Froes F.H., The use of titanium in family automobiles: current trends, *JOM*, 2001, **53** (2): 27.

[7] Esteban P.G., Ruiz-Navas E.M., and Bolzon L., Low-cost titanium alloys? Iron may hold the answers, *Met. Pow. Rep.*, 2008, **63** (4): 24.

[8] Kawabe Y., Research activities on cost effective metallurgy of titanium alloys in Japan, [in] *Proc. of 9th World Conference on Titanium*, Russia, 1999: 1275.

[9] Li Z., and Sun J.K., Development and applications of low cost titanium alloys, *Rare Met. Mater. Eng.*, 2008, **37** (s3): 973.

[10] Bhattacharjee A., Ghosal P., Gogia A.K., Bhargava S., and Kamat S.V., Room temperature plastic flow behaviour of Ti–6.8Mo–4.5Fe–1.5Al and Ti–10V–4.5Fe–1.5Al: effect of grain size and strain rate, *Mater. Sci. Eng., A*, 2007, **452-453**: 219.

[11] Seagle S.R., The state of the USA titanium industry in 1995, *Mater. Sci. Eng., A*, 1996, **213** (1-2): 1.

[12] Ogawa M., Research and developement of low cost titanium alloys, *J. Jpn. Inst. Light Met.*, 2005, **55** (11): 549.

[13] Zhao Y.Q., Li Y.L., Wu H., Zhu K.Y., and Liu C.L., Research on low cost titanium alloys, *Chin. J. Rare Met.*, 2004, **28** (1): 66.

[14] Gunawarman B., Niinomi M., Akahori T., Souma T., Ikeda M., Toda H., and Terashima K., Fatigue characteristics of low cost β titanium alloys for healthcare and medical applications, *Mater. Trans. JIM.*, 2005, **46** (7): 1570.

[15] Gunawarman B., Niinomi M., Akahori T., Souma T., Ikeda M., and Toda H., Mechanical properties and microstructures of low cost β titanium alloys for healthcare applications, *Mater. Sci. Eng., C*, 2005, **25** (3): 304.

[16] Zeng W.D., and Zhou Y.G., Influence of cooling rate on microstructure and mechanical properties of beta processed TC11 alloy, *Acta Metal. Sin.*, 2002, **38** (12): 1273.

[17] Ikeda M., Komatsu S., Ueda M., and Suzuki A., The effect of cooling rate from solution treatment temperature on phase constitution and tensile properties of Ti-4.3Fe-7.1Cr-3.0Al alloy, *Mater. Trans. JIM.*, 2004, **45** (5): 1566.

[18] Xin S.W., Zhao Y.Q., and Zeng W.D., Mechanism of V and Cr on mechanical properties of Ti40 burn resistant titanium alloy, *Chin. J. Nonferrous Met.*, 2008, **18** (7): 1216.

[19] Ng H.P., Douguet E., Bettles C.J., and Muddle B.C., Age-hardening behaviour of two metastable beta-titanium alloys, *Mater. Sci. Eng., A*, 2010, **527** (27): 7017.

[20] Lou G.T., Sun J.K., Yang X.D., Chen L.P., Wang B., and Chen C.H., Effects of Al and Mo on mechanical properties of cast titanium alloys, *Dev. Appl. Mater.*, 2003, **18** (4): 32.